Journal of Hazardous Materials 107 (2004) 27–36

Journal of Hazardous Materials

www.elsevier.com/locate/jhazmat

Modeling evaporation using models that are not boundary-layer regulated

Merv F. Fingas*

Emergencies Science and Technology Division, Environment Canada, Ottawa, Ont. Canada

Abstract

Experimentation shows that oil is not strictly air boundary-layer regulated. The fact that oil evaporation is not strictly boundary-layer regulated implies that a simplistic evaporation equation suffices to describe the process. The following processes do not require consideration: wind velocity, turbulence level, area, thickness, and scale size. The factors important to evaporation are time and temperature.

The equation parameters found experimentally for the evaporation of oils can be related to commonly available distillation data for the oil. Specifically, it has been found that the distillation percentage at 180 °C correlates well with the equation parameters. Relationships have been developed enabling calculation of evaporation equations directly from distillation data:

$$\text{percentage evaporated} = 0.165(\%D)\ln(t) \quad (1)$$

where $\%D$ is the percentage (by weight) distilled at 180 °C and t is the time in minutes.

These equations were combined with the equations generated to account for the temperature variations:

$$\text{percentage evaporated} = [0.165(\%D) + 0.045(T - 15)]\ln(t) \quad (2)$$

The results have application in oil spill prediction and modeling. The simple equations can be applied using readily available data such as sea temperature and time. Old equations required oil vapour pressure, specialized distillation data, spill area, wind speed, and mass transfer coefficients, all of which are difficult to obtain.

Keywords: Evaporation; Oil evaporation; Oil spills; Boundary-layer evaporation; Weathering

1. Introduction

Evaporation is a very important process for most oil spills. In a few days, typical crude oils can lose up to 40% of their volume [1]. Most oil spill behaviour models include evaporation as a process and in the output of the model. Despite the importance of the process, relatively little work has been conducted on the basic physics and chemistry of oil spill evaporation [2]. The difficulty with oil evaporation is that oil is a mixture of hundreds of compounds and this mixture varies from source to source and even over time. Much of the work described in the literature focuses on 'calibrating' equations developed for water evaporation [2]. Furthermore, very little empirical data on oil evaporation has been published in the past.

Scientific and quantitative work on water evaporation is decades old [3,4]. The basis for the oil work in the literature is water evaporation. There are several fundamental differences between the evaporation of a pure liquid such as water and that of a multi-component system such as crude oil. Most obviously, the evaporation rate for a single liquid such as water is a constant with respect to time [3,4]. Evaporative loss, by total weight or volume, is not linear with time for crude oils and other multi-component fuel mixtures [5].

Evaporation of a liquid can be considered as the movement of molecules from the surface into the vapour phase above it. The layer of air above the evaporation surface is known as the boundary layer [6]. The characteristics of this air layer or boundary layer can influence evaporation. In the case of water, the boundary layer regulates the evaporation rate. Air can hold a variable amount of water, depending on temperature, as expressed by the relative humidity. Under conditions where the boundary layer is not moving (no

* Tel.: +613-998-9622; fax: +613-991-9485.
E-mail address: fingas.merv@etc.ec.gc.ca (M.F. Fingas).

0304-3894/$ – see front matter © 2003 Elsevier B.V. All rights reserved.
doi:10.1016/j.jhazmat.2003.11.007

wind) or has low turbulence, the air immediately above the water quickly becomes saturated and evaporation slows or ceases. In practice, the actual evaporation of water proceeds at a small fraction of the possible rate because of the saturation of the boundary layer. The boundary-layer physics is then said to regulate the evaporation of water. This regulation manifests itself in the sensitivity of evaporation to wind or turbulence. When turbulence is weak or absent, evaporation can slow down by orders-of-magnitude. The molecular diffusion of water molecules is at least 10^3 times slower than turbulent diffusion [6].

Evaporation can be viewed as consisting of two components, fundamental evaporation and regulation mechanisms. Fundamental evaporation is that process consisting of the evaporation of the liquid directly into the vapour phase without any regulation other than by the thermodynamics of the liquid itself. Regulation mechanisms are those processes that serve to regulate the final evaporation rate into the environment. For water, the main regulation factor is the air boundary-layer regulation discussed above. The boundary-layer regulation is manifested by the limited rate of diffusion, both molecular and turbulent diffusion, and by saturation dynamics. Molecular diffusion is based on exchange of molecules over the mean free path in the gas. The rate of molecular diffusion for water is about 10^5 slower than the maximum rate of evaporation possible, purely from thermodynamic considerations [6]. The rate for turbulent diffusion, the combination of molecular diffusion and movement with turbulent air, is on the order of 10^2 slower than that for maximum evaporation. In fact, in the case of water, maximum evaporation is not known and has only been estimated by experiments in artificial environments or by calculation [3].

If the evaporation of oil was like that of water and was boundary-layer regulated one could write the mass transfer rate in semi-empirical form (also in generic and unitless form) as:

$$E \approx KCT_u S \tag{3}$$

where E is the evaporation rate in mass per unit area, K the mass transfer rate of the evaporating liquid, presumed constant for a given set of physical conditions, sometimes denoted as k_g (gas phase mass transfer coefficient, which may incorporate some of the other parameters noted here), C the concentration (mass) of the evaporating fluid as a mass per volume, T_u a factor characterizing the relative intensity of turbulence, and S a factor that relates to the saturation of the boundary layer above the evaporating liquid. The saturation parameter, S, represents the effects of local advection on saturation dynamics. If the air is already saturated with the compound in question, the evaporation rate approaches zero. This also relates to the scale length of an evaporating pool. If one views a large pool over which a wind is blowing, there is a high probability that the air is saturated downwind and the evaporation rate per unit area is lower than for a smaller pool. It should be noted that there any many equivalent ways of expressing this fundamental evaporation equation.

Much of the pioneering work for evaporation work was performed by Sutton [7]. Sutton proposed an equation based largely on empirical work:

$$E = KC_s U^{7/9} d^{-1/9} Sc^{-r} \tag{4}$$

where C_s is the concentration of the evaporating fluid (mass/volume), U the wind speed, d the area of the pool, Sc the Schmidt number and r the empirical exponent assigned values from 0 to 2/3. Other parameters are defined as above. The terms in this equation are analogous to the very generic Eq. (1), proposed above. The turbulence is expressed by a combination of the wind speed, U, and the Schmidt number, Sc. The Schmidt number is the ratio of kinematic viscosity of air (ν) to the molecular diffusivity (D) of the diffusing gas in air, i.e., a dimensionless expression of the molecular diffusivity of the evaporating substance in air. The coefficient of the wind power typifies the turbulence level. The value of 0.78 (7/9) as chosen by Sutton, represents a turbulent wind whereas a coefficient of 0.5 would represent a wind flow that was more laminar. The scale length is represented by d and has been given an empirical exponent of $-1/9$. This represents, for water, a weak dependence on size. The exponent of the Schmidt number, r, represents the effect of the diffusivity of the particular chemical, and historically was assigned values between 0 and 2/3 [7].

This expression for water evaporation was subsequently used by those working on oil spills to predict and describe oil and petroleum evaporation. Much of the literature follows the work of Mackay and co-workers [5,8]. Mackay and co-workers adapted the equations for hydrocarbons using the evaporation rate of cumene. Data on the evaporation of water and cumene have been used to correlate the gas phase mass transfer coefficient as a function of wind speed and pool size by the equation:

$$K_m = 0.0292 U^{0.78} X^{-0.78} Sc^{-0.67} \tag{5}$$

where K_m is the mass transfer coefficient in units of mass per unit time and X the pool diameter or the scale size of evaporating area. Stiver and Mackay [5] subsequently developed this further by adding a second equation:

$$N = \frac{k_m AP}{RT} \tag{6}$$

where N is the evaporative molar flux (mol/s), k_m the mass transfer coefficient at the prevailing wind (m/s), A the area (m^2), P the vapour pressure of the bulk liquid (Pa), R the gas constant (8.314 J/(mol K)), and T the temperature (K).

Thus, boundary-layer regulation was assumed to be the primary regulation mechanism for oil and petroleum evaporation. This assumption was never tested by experimentation, as revealed by the literature search [2]. The implications of these assumptions are that evaporation rate for a given oil is increased by:

- increasing turbulence;
- increasing wind speed; and
- increasing the surface area of a given mass of oil.

These factors can then be verified experimentally to test whether oil is boundary-layer regulated or not. These factors formed the basis of experimentation for this paper.

2. Experimental

Detailed experimental results are given in the literature [9].

Evaporation rate was measured by weight loss using an electronic balance. The balance was a Mettler PM4000. The weight was recorded using a Toshiba 3100, a serial cable to the balance and a modified version of the software program, 'Collect' (Labtronics, Richmond, Ont.).

Measurements were conducted in the following fashion. A tared petri dish of defined size was loaded with a measured amount of oil. At the end of the experiment, vessels were cleaned and rinsed with dichloromethane and a new experiment started. The weight loss dishes were standard glass petri dishes from Corning. A standard 139 mm diameter (i.d.) dish was used for most experiments. For the experiments in which area was a variable, dishes of other diameters were used.

The constant temperature chamber (room) used was a constant temperature model constructed in 1993. It could maintain temperatures from −40 to +60 °C and regulate the chosen temperature within ±1 °C.

In experiments involving wind, air velocities were measured using a Taylor vane anemometer (no model number on the unit) and a Tadi, 'Digital Pocket Anemometer'. Details of these measurements are given in the literature [9]. These velocities were later confirmed using a hot wire anemometer and appropriate data manipulations of the outputs. The anemometer was a Thermo Systems (TSI) model 1053b, with power supply (TSI model 1051-1), averaging circuit (TSI model 1047), and signal linearlizing circuit (TSI model 1052). The voltage from the averaging circuit was read with a Fluke 1053 voltmeter. The hot wire sensor (TSI model 1213-60) was angled at 45°.

Evaporation data were collected on the Toshiba 3100 laptop computer and subsequently transferred to other computers for analysis. Curve fitting was performed using the software program "TableCurve", Jandel Scientific Corporation, San Raphael, CA.

Oils were taken from supplies of Environment Canada and were supplied by various oil companies for environmental testing. Properties of the oils can be found in standard references [10].

3. Results and discussion

The results of the boundary-regulation experiments are presented in the order of the experimental series.

3.1. Wind experiments

Experiments on the evaporation of oil with and without wind were conducted with Alberta Sweet Mixed Blend (ASMB), gasoline, and with water. Water formed a baseline data set since much is known about its evaporation behaviour [11]. Regressions on the data were performed and the equation parameters calculated. Curve coefficients are the constants from the best fit equation [Evap $= a\ln(t)$], t: time in minutes, for logarithmic equations or Evap $= a\sqrt{t}$, for the square root equations. Oils with few components evaporating at one time have a tendency to fit square root curves [12]. While data were calculated separately for percentage of weight lost and absolute weight, the latter is usually used because it is more convenient. Both values show the small relative upward tendency with respect to wind effects. The plots of wind speed versus the evaporation rate (as a percentage of weight lost) for each oil type, are shown in Figs. 1–3. These figures show that the evaporation rates for oils and even the light product, gasoline and water are not increased by a significant amount with increasing wind speed. In most cases, there is a rise from the 0-wind level to the 1 m/s level, but after that, the rate remains relatively constant. The evaporation rate after the 0-wind value is nearly identical for all oils. The oil evaporation data can be compared to the evaporation of water, as illustrated in Fig. 3. These data show the classical relationship of the water evaporation rate correlated with the wind speed (evaporation varies as $U^{0.78}$, where U is wind speed). This, by itself, would appear to indicate that the oils used here are somewhat boundary-layer regulated, but only to the degree that the effect is seen in moving from 0-wind to 1 m/s, and not thereafter.

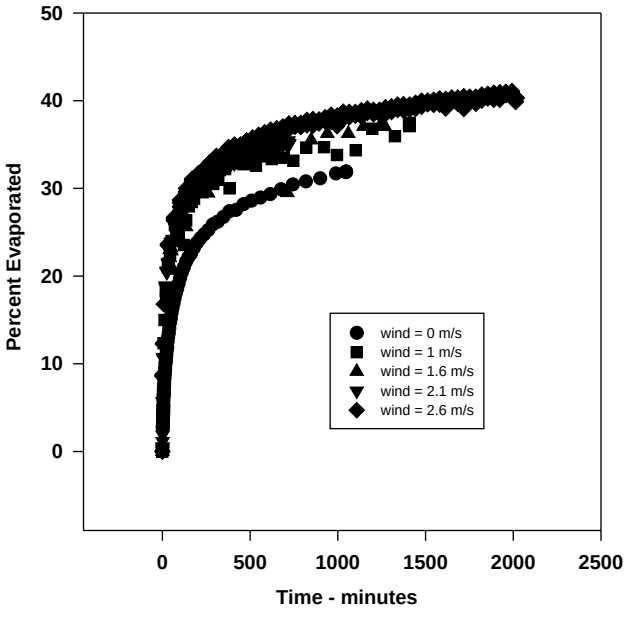

Fig. 1. Evaporation of ASMB with varying wind velocities.

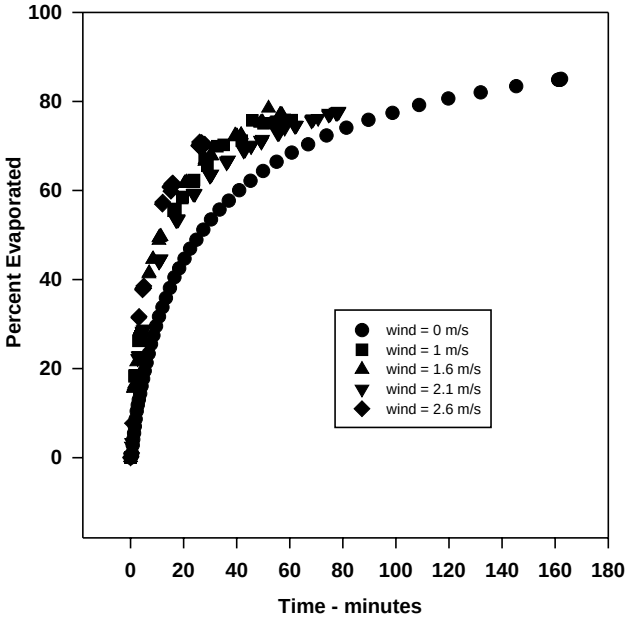

Fig. 2. Evaporation of gasoline with varying wind velocities.

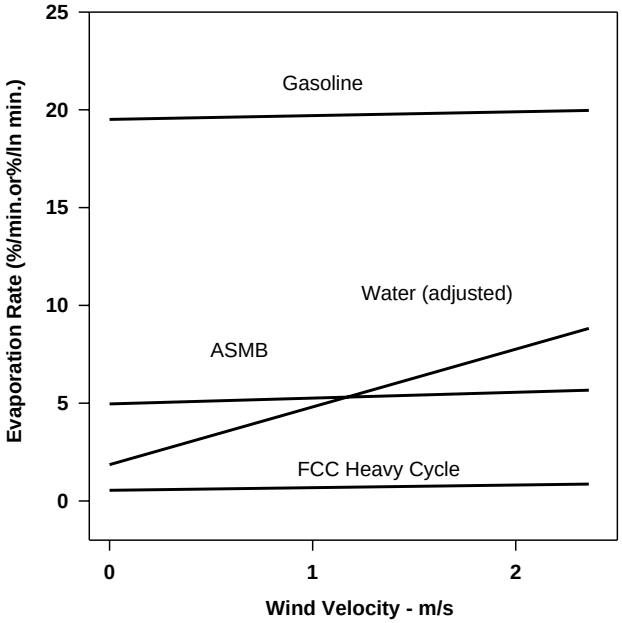

Fig. 4. Correlation of evaporation rates and wind velocity.

Fig. 4 shows the rates of evaporation compared to the wind speed for all the liquids used in this study. This figure shows the evaporation rates of all test liquids versus wind speed. The lines shown are those calculated by linear regression using the graphics software, Sigma Plot. This clearly shows that water evaporation rate increased, as expected, with increasing wind velocity. The oils, ASMB and gasoline, do not show a significant increase with increasing wind speed. The increase may only be a result of the increase in evaporation in going from the 0-wind level to the other levels. In any case, they do not show the $U^{0.78}$ relationship that water shows.

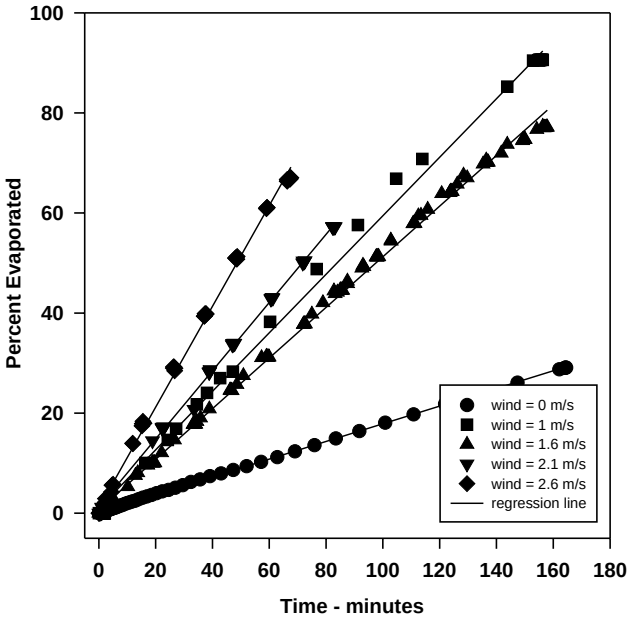

Fig. 3. Evaporation of water with varying wind velocities.

All the above data show that oil is only slightly, if at all, boundary-layer regulated, perhaps only affecting the very initial rates after turbulence is applied.

3.2. Evaporation rate and area

Alberta Sweet Mixed Blend was also used to conduct a series of experiments with varying evaporation area. The mass of the oil was kept constant so that the thickness of the oil would also vary. However, the greater the area, the lesser the thickness and both factors would increase oil evaporation if it were boundary-layer regulated. Data are illustrated graphically in Fig. 5. These data show, at best, a very weak correlation of thickness and area with evaporation rate. Because of the poor correlation between area and evaporation rate, one can conclude that evaporation rate is not highly correlated with area and that the evaporation of oil is not boundary-layer regulated to any significant degree.

3.3. Study of mass and evaporation rate

Alberta Sweet Mixed Blend oil was again used to conduct a series of experiments with volume as the major variant. Alternatively, thickness and area were held constant to ensure that the strict relationship between these two variables did not affect the final regression results. Fig. 6 illustrates the relationship between evaporation rate and volume of evaporation material (also equivalent to mass of evaporating material). This figure illustrates a strong correlation between oil mass (or volume) and evaporation rate. This suggests no or little boundary-layer regulation. It also shows that any tendencies observed in the area tests described above may have been due to volume/mass factors rather than area.

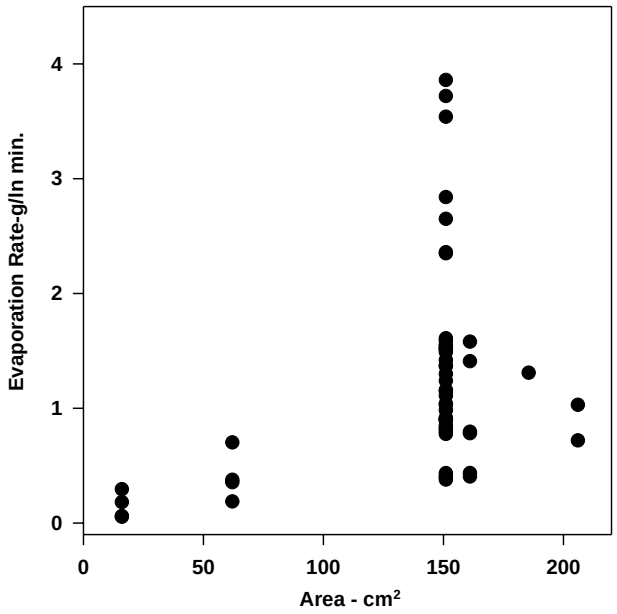

Fig. 5. Correlation of area with evaporation rate.

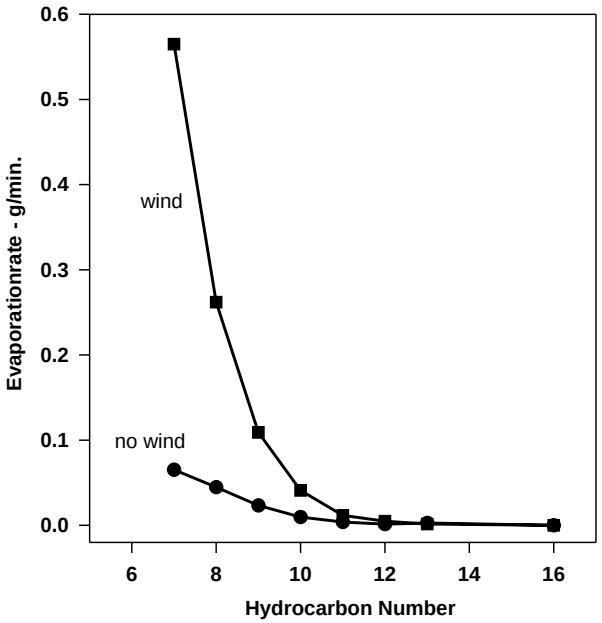

Fig. 7. Evaporation Rate of pure compounds.

3.4. Study of the evaporation of pure hydrocarbons—with and without wind

A study of the evaporation rate of pure hydrocarbons was conducted to test the classic boundary-layer evaporation theory as applied to the hydrocarbon constituents of oils. The evaporation rate data are illustrated in Fig. 7. This figure shows that the evaporation rates of the pure hydrocarbons have a variable response to wind. Heptane (hydrocarbon number 7) shows a large difference between evaporation rate in wind and no wind conditions, indicating boundary-layer regulation. Decane (carbon number 10) shows a lesser effect and hexadecane (carbon number 16) shows a negligible difference between the two experimental conditions. This experiment shows the extent of boundary-regulation and the reason for the small or negligible degree of boundary-regulation shown by crude oils and petroleum products. Crude oil contains very little material with carbon numbers less than decane, often less than 3% of its composition [11]. Even the more volatile petroleum products, gasoline and diesel fuel only have limited amounts of compounds more volatile than decane, and thus are also not strongly boundary-layer regulated.

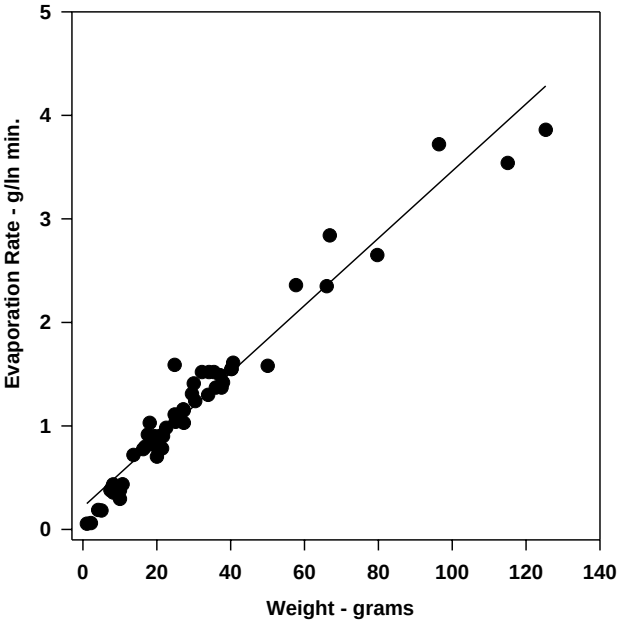

Fig. 6. Correlation of mass with evaporation rate.

Another evaluation of evaporation regulation is that of saturation concentration, the maximum concentration soluble in air. The saturation concentrations of water and several oil components are listed in Table 1 [13]. This table shows that saturation concentration of water is less than that of many

Table 1
Saturation concentration of water and hydrocarbons

Substance	Saturation concentration at 25 °C (g/m^3)[a]
Water	20
n-Pentane	1689
Hexane	564
Cyclohexane	357
Benzene	319
n-Heptane	196
Methylcyclohexane	192
Toluene	110
Ethybenzene	40
p-Xylene	38
m-Xylene	35
o-Xylene	29

[a] Values taken from Ullmann's Encyclopedia.

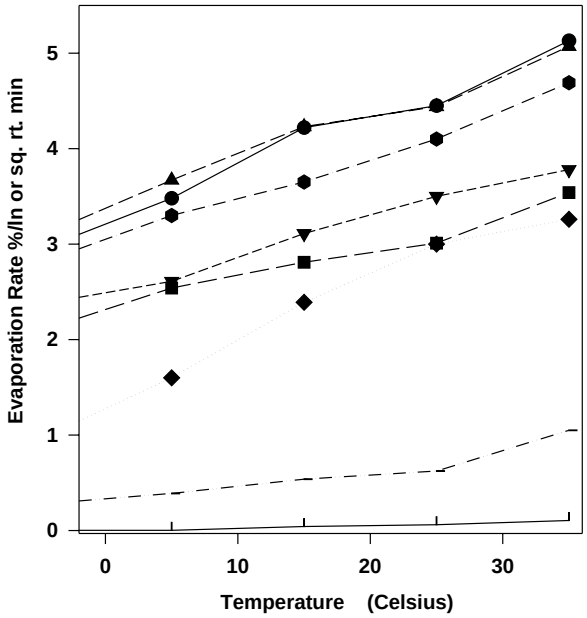

Fig. 8. Variation of evaporation rates with temperature.

common oil components. The saturation concentration of water is in fact, about two orders-of-magnitude less than the saturation concentration of volatile oil components such as pentane. This further explains why oil has a boundary-layer limitation higher than that of water.

Fig. 8 shows the composite of all evaporation rates versus temperature. The evaporation rates are the coefficients of the logarithmic equation except for diesel and Bunker C Light, for which they are the coefficients of the square root equation. Fig. 8 shows that the evaporation rates (used here interchangeably with equation parameters) are linear with respect to temperature. This confirms the theoretical approaches discussed in the introduction above. These show the evaporation rates with curves fit by linear regression. The curves for the light crudes, ASMB, Brent, Arabian Light, Statfjord, and Gullfaks appear to be parallel. The curves for gasoline, Terra Nova crude, diesel, and Bunker C Light have different slopes than those for crude oils, which may be due to the unique properties of these liquids. Gasoline evaporates at a rapid rate and is composed of only lighter crude components. Terra Nova is a heavier crude with a large wax component. Diesel is a refined fuel with medium to heavy components remaining. Bunker C Light is a refined residual with a small amount of diesel as a diluent. The evaporation rates of the latter two products are best fit with square root equations rather than logarithmic equations.

Further examination of the temperature behaviour of oil evaporation was conducted by determining the equations by which the evaporation rates, or equation parameters, change with temperature. A series of correlations was performed, between the evaporation rates, by both percentage and weight loss, using a linear equation.

The resulting finding that unique equations may be needed for each oil is a significant disadvantage to practical end use, and a way to accurately predict evaporation using other readily available data is necessary. Two means to predict the evaporation were developed. The first data type is to use the value of the slope (fitted with one parameter) at 15 °C as a basis for correlation. The assumption here is that the slopes of the temperature parameters are similar, so that they can be used as a predictor. It has already been noted that only light and medium crude oils display similar slopes. However, it will be fruitful to test such a hypothesis. The other observation noted is that the slope of the equation appears to correlate with the magnitude of the evaporation rate at 15 °C. The second type of data used to study evaporation are distillation data. Distillation data are very common and are often the only data used to characterize oils. This is because the data are crucial in operating refineries. Crudes may even be priced on the basis of their distillation data. New procedures to measure distillation data are very simple, fast and repeatable [10]. Two separate ways of using the distillation data will be tried, first a portion of the curve, and second, the entire distillation curve slope.

The empirically measured parameters at 15 °C were correlated with both the slopes and the intercepts of the temperature equations. Full details of this correlation are given in the literature [1]. The resulting equations are:

$$\text{percentage evaporated} = [B + 0.045(T - 15)] \quad (7)$$

where B is the equation parameter at 15 °C and T the temperature in degrees Celsius.

Distillation data were directly correlated to the evaporation rates determined by experimentation. The distillation data are available in two forms, percent evaporated at a given temperature value (as used here) and as temperature at which a fixed amount of material is lost. The percentage distilled at each temperature was correlated with the equation parameter (sometimes referred to here as the evaporation rate). Detailed correlation data are given in the literature [1]. The optimal point, or point at which the regression coefficient is maximum, was found to be 180 °C by using peak functions. The percent mass distilled at 180° was used to calculate the relationship between the distillation values and the equation parameters. The equations used were derived from correlations of the data.

The data from those oils that were better fitted with square root equations—diesel, Bunker C Light and FCC Heavy Cycle—were separated and calculated separately. Since there are only three data points, the reliability and accuracy are lower than for the other set.

The equations derived from the regressions are as follows:

For oils that follow a logarithmic equation:

$$\text{percentage evaporated} = 0.165(\%D)\ln(t) \quad (8)$$

For oils that follow a square root equation:

$$\text{percentage evaporated} = 0.0254(\%D)\sqrt{t} \quad (9)$$

where $\%D$ is the percentage (by weight) distilled at 180 °C.

Table 2
Empirical equations for predicting evaporation

Oil type	Equation	Oil type	Equation	Oil type	Equation
Adgo	$\%Ev = (0.11 + 0.013T)\sqrt{t}$	FCC Medium Cycle	$\%Ev = (-0.16 + 0.013T)\sqrt{t}$	Orimulsion plus water	$\%Ev = (3 + 0.045T)\ln(t)$
Adgo—long term	$\%Ev = (0.68 + 0.045T)\ln(t)$	FCC-VGO	$\%Ev = (2.5 + 0.013T)\sqrt{t}$	Oseberg	$\%Ev = (2.68 + 0.045T)\ln(t)$
Alberta Sweet Mixed Blend	$\%Ev = (3.24 + 0.054T)\ln(t)$	Federated	$\%Ev = (3.47 + 0.045T)\ln(t)$	Panuke	$\%Ev = (7.12 + 0.045T)\ln(t)$
Amauligak	$\%Ev = (1.63 + 0.045T)\ln(t)$	Federated (new—1999)	$\%Ev = (3.45 + 0.045T)\ln(t)$	Pitas Point	$\%Ev = (7.04 + 0.045T)\ln(t)$
Amauligak—f24	$\%Ev = (1.91 + 0.045T)\ln(t)$	Garden Banks 387	$\%Ev = (1.84 + 0.045T)\ln(t)$	Platform Gail (Sockeye)	$\%Ev = (1.68 + 0.045T)\ln(t)$
Arabian Medium	$\%Ev = (1.89 + 0.045T)\ln(t)$	Garden Banks 426	$\%Ev = (3.44 + 0.045T)\ln(t)$	Platform Holly	$\%Ev = (1.09 + 0.045T)\ln(t)$
Arabian Heavy	$\%Ev = (1.31 + 0.045T)\ln(t)$	Gasoline	$\%Ev = (13.2 + 0.21T)\ln(t)$	Platform Irene—long term	$\%Ev = (0.74 + 0.045T)\ln(t)$
Arabian Heavy	$\%Ev = (2.71 + 0.045T)\ln(t)$	Genesis	$\%Ev = (2.12 + 0.045T)\ln(t)$	Platform Irene—short term	$\%Ev = (-0.05 + 0.013T)\sqrt{t}$
Arabian Light	$\%Ev = (2.52 + 0.037T)\ln(t)$	Green Canyon Block 109	$\%Ev = (1.58 + 0.045T)\ln(t)$	Point Arguello—co-mingled	$\%Ev = (1.43 + 0.045T)\ln(t)$
Arabian Light	$\%Ev = (3.41 + 0.045T)\ln(t)$	Green Canyon Block 184	$\%Ev = (3.55 + 0.045T)\ln(t)$	Point Arguello Heavy	$\%Ev = (0.94 + 0.045T)\ln(t)$
Arabian Light (2001)	$\%Ev = (2.4 + 0.045T)\ln(t)$	Green Canyon Block 65	$\%Ev = (1.56 + 0.045T)\ln(t)$	Point Arguello Light	$\%Ev = (2.44 + 0.045T)\ln(t)$
ASMB—Standard #5	$\%Ev = (3.35 + 0.045T)\ln(t)$	Greenplus Hydraulic Oil	$\%Ev = (-0.68 + 0.045T)\ln(t)$	Point Arguello Light—b	$\%Ev = (2.3 + 0.045T)\ln(t)$
ASMB (offshore)	$\%Ev = (2.2 + 0.045T)\ln(t)$	Greenplus Hydraulic Oil	$\%Ev = (-0.68 + 0.045T)\ln(t)$	Polypropylene Tetramer	$\%Ev = (0.25)(t)$ (at 15 °C)
Av Gas 80	$\%Ev = (15.4 + 0.045T)\ln(t)$	Gullfaks	$\%Ev = (2.29 + 0.034T)\ln(t)$	Port Hueneme	$\%Ev = (0.3 + 0.045T)\ln(t)$
Avalon	$\%Ev = (1.41 + 0.045T)\ln(t)$	Heavy Reformate	$\%Ev = (-0.17 + 0.013T)\sqrt{t}$	Prudhoe Bay (old stock)	$\%Ev = (1.69 + 0.045T)\ln(t)$
Avalon J-34	$\%Ev = (1.58 + 0.045T)\ln(t)$	Hebron MD-4	$\%Ev = (1.01 + 0.045T)\ln(t)$	Prudhoe Bay (new stock)	$\%Ev = (2.37 + 0.045T)\ln(t)$
Aviation Gasoline 100 LL	$\ln(\%Ev) = (0.5 + 0.045T)\ln(t)$	Heidrun	$\%Ev = (1.95 + 0.045T)\ln(t)$	Prudhoe stock b	$\%Ev = (1.4 + 0.045T)\ln(t)$
Barrow Island	$\%Ev = (4.67 + 0.045T)\ln(t)$	Hibernia	$\%Ev = (2.18 + 0.045T)\ln(t)$	Rangely	$\%Ev = (1.89 + 0.045T)\ln(t)$
BCF-24	$\%Ev = (1.08 + 0.045T)\ln(t)$	High Viscosity Fuel Oil	$\%Ev = (-0.12 + 0.013T)\sqrt{t}$	Sahara Blend	$\%Ev = (0.001 + 0.013T)\sqrt{t}$
Belridge Crude	$\%Ev = (0.03 + 0.013T)\sqrt{t}$	Hondo	$\%Ev = (1.49 + 0.045T)\ln(t)$	Sahara Blend (long term)	$\%Ev = (1.09 + 0.045T)\ln(t)$
Bent Horn A-02	$\%Ev = (3.19 + 0.045T)\ln(t)$	Hout	$\%Ev = (2.29 + 0.045T)\ln(t)$	Sakalin	$\%Ev = (4.16 + 0.045T)\ln(t)$
Beta	$\%Ev = (-0.08 + 0.013T)\sqrt{t}$	IFO-180	$\%Ev = (-0.12 + 0.013T)\sqrt{t}$	Santa Clara	$\%Ev = (1.63 + 0.045T)\ln(t)$
Beta—long term	$\%Ev = (0.29 + 0.045T)\ln(t)$	IFO-30 (Svalbard)	$\%Ev = (-0.04 + 0.045T)\ln(t)$	Scotia Light	$\%Ev = (6.87 + 0.045T)\ln(t)$
Boscan	$\%Ev = (-0.15 + 0.013T)\sqrt{t}$	IFO-300 (old Bunker C)	$\%Ev = (-0.15 + 0.013T)\sqrt{t}$	Scotia Light	$\%Ev = (6.92 + 0.045T)\ln(t)$
Brent	$\%Ev = (3.39 + 0.048T)\ln(t)$	Iranian Heavy	$\%Ev = (2.27 + 0.045T)\ln(t)$	Ship Shoal Block 239	$\%Ev = (2.71 + 0.045T)\ln(t)$
Bunker C—Light (IFO-250)	$\%Ev = (.0035 + 0.0026T)\sqrt{t}$	Jet A1	$\%Ev = (0.59 + 0.013T)\sqrt{t}$	Ship Shoal Block 269	$\%Ev = (3.37 + 0.045T)\ln(t)$
Bunker C—long term	$\%Ev = (-0.21 + 0.045T)\ln(t)$	Jet Fuel (Anch)	$\%Ev = (7.19 + 0.045T)\ln(t)$	Sockeye	$\%Ev = (2.14 + 0.045T)\ln(t)$
Bunker C—short term)	$\%Ev = (0.35 + 0.013T)\sqrt{t}$	Jet Fuel (Anch) short term	$\%Ev = (1.06 + 0.013T)\sqrt{t}$	Sockeye Co-mingled	$\%Ev = (1.38 + 0.045T)\ln(t)$
Bunker C Anchorage	$\%Ev = (-0.13 + 0.013T)\sqrt{t}$	Issungnak	$\%Ev = (1.56 + 0.045T)\ln(t)$	Sockeye Sour	$\%Ev = (1.32 + 0.045T)\ln(t)$
Bunker C Anchorage (long term)	$\%Ev = (0.31 + 0.045T)\ln(t)$	Isthmus	$\%Ev = (2.48 + 0.045T)\ln(t)$	Sockeye Sweet	$\%Ev = (2.39 + 0.045T)\ln(t)$
California API 11	$\%Ev = (-0.13 + 0.013T)\sqrt{t}$	Jet 40 Fuel	$\%Ev = (8.96 + 0.045T)\ln(t)$	South Louisiana	$\%Ev = (2.39 + 0.045T)\ln(t)$
California API 15	$\%Ev = (-0.14 + 0.013T)\sqrt{t}$	Jet A1	$\%Ev = (.59 + 0.013T)\sqrt{t}$	South Pass Block 60	$\%Ev = (2.91 + 0.045T)\ln(t)$

Table 2 (*Continued*)

Oil type	Equation	Oil type	Equation	Oil type	Equation
Cano Limon	$\%Ev = (1.71 + 0.045T)\ln(t)$	Jet Fuel (Anch)	$\%Ev = (7.19 + 0.045T)\ln(t)$	South Pass Block 67	$\%Ev = (2.17 + 0.045T)\ln(t)$
Canola Oil	Little	Jet Fuel (Anch) short term	$\%Ev = (1.06 + 0.013T)\sqrt{t}$	South Pass Block 93	$\%Ev = (1.5 + 0.045T)\ln(t)$
Carpenteria	$\%Ev = (1.68 + 0.045T)\ln(t)$	Komineft	$\%Ev = (2.73 + 0.045T)\ln(t)$	South Timbalier Block 130	$\%Ev = (2.77 + 0.045T)\ln(t)$
Cat cracking feed	$\%Ev = (-0.18 + 0.013T)\sqrt{t}$	Lago	$\%Ev = (1.13 + 0.045T)\ln(t)$	Soybean oil	Little
Chavyo	$\%Ev = (3.52 + 0.045T)\ln(t)$	Lago Treco	$\%Ev = (1.12 + 0.045T)\ln(t)$	Statfjord	$\%Ev = (2.67 + 0.06T)\ln(t)$
Combined oil/gas	$\%Ev = (-0.08 + 0.013T)\sqrt{t}$	Lucula	$\%Ev = (2.17 + 0.045T)\ln(t)$	Sumatran Heavy	$\%Ev = (-0.11 + 0.013T)\sqrt{t}$
Compressor Lube Oil—new	$\%Ev = (-0.68 + 0.045T)\ln(t)$	Main Pass Block 306	$\%Ev = (2.86 + 0.045T)\ln(t)$	Sumatran Light	$\%Ev = (0.96 + 0.045T)\ln(t)$
Cook Inlet—Granite Point	$\%Ev = (4.54 + 0.045T)\ln(t)$	Main Pass Block 37	$\%Ev = (3.04 + 0.045T)\ln(t)$	Taching	$\%Ev = (-0.11 + 0.013T)\sqrt{t}$
Cook Inlet—Swanson River	$\%Ev = (3.58 + 0.045T)\ln(t)$	Malongo	$\%Ev = (1.67 + 0.045T)\ln(t)$	Takula	$\%Ev = (1.95 + 0.045T)\ln(t)$
Cook Inlet Trading Bay	$\%Ev = (3.15 + 0.045T)\ln(t)$	Marinus Turbine Oil	$\%Ev = (-0.68 + 0.045T)\ln(t)$	Tapis	$\%Ev = (3.04 + 0.045T)\ln(t)$
Corrosion Inhibitor Solvent	$\%Ev = (-0.02 + 0.013T)\sqrt{t}$	Marinus Valve Oil	$\%Ev = (-0.68 + 0.045T)\ln(t)$	Tchatamba Crude	$\%Ev = (3.8 + 0.045T)\ln(t)$
Crude Castor oil	Little	Mars TLP	$\%Ev = (2.18 + 0.045T)\ln(t)$	Terra Nova	$\%Ev = (1.36 + 0.045T)\ln(t)$
Cusiana	$\%Ev = (3.39 + 0.045T)\ln(t)$	Maui	$\%Ev = (-0.14 + 0.013T)\sqrt{t}$	Terresso 150	$\%Ev = (-0.68 + 0.045T)\ln(t)$
Delta West Block 97	$\%Ev = (6.57 + 0.045T)\ln(t)$	Maya	$\%Ev = (1.38 + 0.045T)\ln(t)$	Terresso 220	$\%Ev = (-0.66 + 0.045T)\ln(t)$
Diesel Anchorage—Long	$\%Ev = (4.54 + 0.045T)\ln(t)$	Mayan crude	$\%Ev = (1.45 + 0.045T)\ln(t)$	Terresso 46 Industrial oil	$\%Ev = (-0.67 + 0.045T)\ln(t)$
Diesel Anchorage—Short	$\%Ev = (0.51 + 0.013T)\sqrt{t}$	Mississippi Canyon Block 72	$\%Ev = (2.15 + 0.045T)\ln(t)$	Thevenard Island	$\%Ev = (5.74 + 0.045T)\ln(t)$
Diesel—long term	$\%Ev = (5.8 + 0.045T)\ln(t)$	Mississippi Canyon Block 194	$\%Ev = (2.62 + 0.045T)\ln(t)$	Turbine Oil STO 90	$\%Ev = (-0.68 + 0.045T)\ln(t)$
Diesel Mobile 1997	$\%Ev = (0.03 + 0.013T)\sqrt{t}$	Mississippi Canyon Block 807	$\%Ev = (2.05 + 0.045T)\ln(t)$	Turbine Oil STO 120	$\%Ev = (-0.68 + 0.045T)\ln(t)$
Diesel (regular stock)	$\%Ev = (.31 + 0.018T)\sqrt{t}$	Nektoralik	$\%Ev = (0.62 + 0.045T)\ln(t)$	Udang	$\%Ev = (-0.14 + 0.013T)\sqrt{t}$
Diesel fuel—Southern—long term	$\%Ev = (2.18 + 0.045T)\ln(t)$	Neptune Spar (Viosca Knoll 826)	$\%Ev = (3.75 + 0.045T)\ln(t)$	Udang (long term)	$\%Ev = (0.06 + 0.045T)\ln(t)$
Diesel fuel—Southern—short term	$\%Ev = (-0.02 + 0.013T)\sqrt{t}$	Nerlerk	$\%Ev = (2.01 + 0.045T)\ln(t)$	Vasconia	$\%Ev = (0.84 + 0.045T)\ln(t)$
Diesel Mobile 1997 long-term	$\%Ev = (-0.02 + 0.013T)\sqrt{t}$	Ninian	$\%Ev = (2.65 + 0.045T)\ln(t)$	Viosca Knoll Block 826	$\%Ev = (2.04 + 0.045T)\ln(t)$
Dos Cuadros	$\%Ev = (1.88 + 0.045T)\ln(t)$	Norman Wells	$\%Ev = (3.11 + 0.045T)\ln(t)$	Viosca Knoll Block 990	$\%Ev = (3.16 + 0.045T)\ln(t)$
Ekofisk	$\%Ev = (4.92 + 0.045T)\ln(t)$	North Slope—Middle Pipeline	$\%Ev = (2.64 + 0.045T)\ln(t)$	Voltesso 35	$\%Ev = (-0.18 + 0.013T)\sqrt{t}$
Empire Crude	$\%Ev = (2.21 + 0.045T)\ln(t)$	North Slope—Northern Pipeline	$\%Ev = (2.64 + 0.045T)\ln(t)$	Waxy Light and Heavy	$\%Ev = (1.52 + 0.045T)\ln(t)$
Endicott	$\%Ev = (0.9 + 0.045T)\ln(t)$	North Slope—Southern Pipeline	$\%Ev = (2.47 + 0.045T)\ln(t)$	West Delta Block 30 w/water	$\%Ev = (-0.04 + 0.013T)\sqrt{t}$
Esso Spartan EP-680 Industrial Oil	$\%Ev = (-0.66 + 0.045T)\ln(t)$	Nugini	$\%Ev = (1.64 + 0.045T)\ln(t)$	West Texas Intermediate	$\%Ev = (2.77 + 0.045T)\ln(t)$
Eugene Island 224-condensate	$\%Ev = (9.53 + 0.045T)\ln(t)$	Odoptu	$\%Ev = (4.27 + 0.045T)\ln(t)$	West Texas Intermediate	$\%Ev = (3.08 + 0.045T)\ln(t)$
Eugene Island Block 32	$\%Ev = (0.77 + 0.045T)\ln(t)$	Olive Oil	Little	West Texas Sour	$\%Ev = (2.57 + 0.045T)\ln(t)$
Eugene Island Block 43	$\%Ev = (1.57 + 0.045T)\ln(t)$	Oriente	$\%Ev = (1.32 + 0.045T)\ln(t)$	White Rose	$\%Ev = (1.44 + 0.045T)\ln(t)$
Evendell	$\%Ev = (3.38 + 0.045T)\ln(t)$	Oriente	$\%Ev = (1.57 + 0.045T)\ln(t)$	Zaire	$\%Ev = (1.36 + 0.045T)\ln(t)$
FCC Heavy Cycle	$\%Ev = (.17 + 0.013T)\sqrt{t}$	Orimulsion 400—dewater	$\%Ev = (3.6)\ln(t)$ (at 15 °C)		
FCC Light	$\%Ev = (-0.17 + 0.013T)\sqrt{t}$				

These equations can be combined with the equations generated in previous work [1] to account for the temperature variations:

For oils that follow a logarithmic equation:

$$\text{percentage evaporated} = [0.165(\%D) + 0.045(T - 15)]\ln(t) \quad (10)$$

For oils that follow a square root equation:

$$\text{percentage evaporated} = [0.0254(\%D) + 0.01(T - 15)]\sqrt{t} \quad (11)$$

where $\%D$ is the percentage (by weight) distilled at 180 °C.

In addition, a large number of experiments were performed on oils to directly measure their evaporation curves. The empirical equations that result are given in Table 2.

Since the equations described above require only time and temperature (or at the very worst, the percentage of oil distilled at 180 °C), it is relatively simple to apply these forms of equations. They can also be applied in models as increments where t, the time, becomes the total time and the previous evaporation is subtracted, e.g., if one was modeling the evaporation of Alberta Sweet Mixed Blend oil in the time step from 12 to 15 h. The equation is (from Table 2):

$$\text{percentage evaporation} = (3.24 + 0.054T)\ln(t) \quad (12)$$

Substituting for the temperature of 15 °C and with a time of 12 h or 720 min, we get a percentage of 26.65. With 18 h, we get a percentage of 27.72 with a difference of 1.07%, the amount evaporated in the interval between 15 and 18 h.

The variation of evaporation is illustrated in Fig. 9, which shows the evaporation of two oils, diesel fuel and North Slope Crude, at two temperatures.

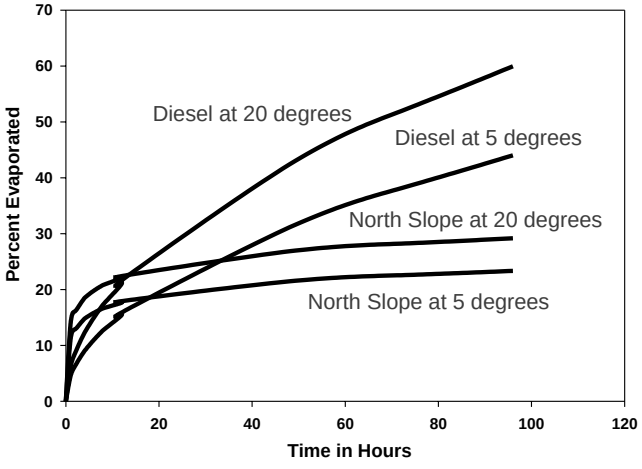

Fig. 9. Comparison of evaporation curves.

4. Conclusions

Oil evaporation is not strictly boundary-layer regulated. The results of the following experimental series have shown the lack of boundary-layer regulation.

(1) A study of the evaporation rate of several oils with increasing wind speed shows that the evaporation rate does not change significantly except for the initial step over the 0-level wind. Water, known to be boundary-layer regulated, does show a significant increase with wind speed, U (U^x, where x varies from 0.5 to 0.78, depending on the turbulence level).
(2) Increasing area does not significantly change the oil evaporation rate. This is directly contrary to the prediction resulting from boundary-layer regulation.
(3) The volume or mass of oil evaporating correlates with the evaporation rate. This is a strong indicator of the lack of boundary-layer regulation because with water, volume (rather than area) and rate do not correlate.
(4) Evaporation of pure hydrocarbons with and without wind (turbulence) shows that compounds larger than nonane and decane are not boundary-layer regulated. Most oil and hydrocarbon products consist of compounds larger than these two and thus would not be expected to be boundary-layer regulated.

The fact that oil evaporation is not strictly boundary-layer regulated implies that a simplistic evaporation equation will suffice to describe the process. The following factors do not require consideration: wind velocity, turbulence level, area, thickness, and scale size. The factors important to evaporation include time and temperature.

The equation parameters found experimentally for the evaporation of oils can be related to commonly available distillation data for the oil. Specifically, it has been found that the distillation percentage at 180 °C correlates well with the equation parameters. Regression coefficients (r^2) range from 0.74 to 0.98, depending on the type of equation and the selection of data [14]. Relationships have been developed that allow evaporation equations to be calculated directly from distillation data.

For oils that follow a logarithmic equation:

$$\text{percentage evaporated} = [0.165(\%D) + 0.045(T - 15)]\ln(t) \quad (13)$$

For oils that follow a square root equation:

$$\text{percentage evaporated} = [0.0254(\%D) + 0.01(T - 15)]\sqrt{t} \quad (14)$$

References

[1] M.F. Fingas, in: Proceedings of the 1999 International Oil Spill Conference, American Petroleum Institute, Washington, DC, 1999, pp. 281–287.
[2] M.F. Fingas, J. Hazard. Mater. 42 (1995) 157.

[3] F.E. Jones, Evaporation of Water, Lewis Publishers, Chelsea, MI, 1992.
[4] W. Brutsaert, Evaporation into the Atmosphere, Reidel Publishing Company, Dordrecht, Holland, 1982.
[5] W. Stiver, D. Mackay, Environ. Sci. Technol. 18 (1984) 834.
[6] J.L. Monteith, M.H. Unsworth, Principles of Environmental Physics, Hodder and Stoughton, London, 1990.
[7] O.G. Sutton, Proc. R. Soc. London, Ser. A 146 (1934) 701.
[8] D. Mackay, R.S. Matsugu, Can. J. Chem. Eng. 51 (1973) 434.
[9] M.F. Fingas, J. Hazard. Mater. 57 (1998) 41.
[10] P.S. Jokuty, S. Whiticar, Z. Wang, M.F. Fingas, B. Fieldhouse, P. Lambert, J. Mullin, Properties of Crude Oils and Oil Products, Environment Canada Manuscript Report EE-165, Ottawa, Ont., 1999.
[11] Z. Wang, M. Fingas, K. Li, J. Chromatogr. Sci. 32 (1994) 361.
[12] M.F. Fingas, J. Hazard. Mater. 56 (1997) 227.
[13] Ullmann Encyclopedia, Ullmann Publishing, Hamburg, 1989–1995.
[14] M.F. Fingas, in: Proceedings of the Nineteenth Arctic and Marine Oil Spill Program Technical Seminar, Environment Canada, Ottawa, Ont., 1996, pp. 29–72.